J Electr Eng Technol.2018; 13(1): 418-429
http://doi.org/10.5370/JEET.2018.13.1.418

ISSN(Print) 1975-0102
ISSN(Online) 2093-7423

Torque Sensorless Decentralized Position/Force Control for Constrained Reconfigurable Manipulator via Non-fragile H_∞ Dynamic Output Feedback

Fan Zhou*, Bo Dong* and Yuanchun Li†

Abstract – This paper studies the decentralized position/force control problem for constrained reconfigurable manipulator without torque sensing. A novel joint torque estimation scheme that exploits the existing structural elasticity of the manipulator joint with harmonic drive model is applied for each joint module. Based on the estimated joint torque and dynamic output feedback technique, a decentralized position/force control strategy is presented. In order to solve the problem of controller parameter perturbation, the non-fragile robust technique is introduced into the dynamic output feedback controller. Subsequently, the stability of the closed-loop system is proved using the Lyapunov theory and linear matrix inequality (LMI) technique. Finally, two 2-DOF constrained reconfigurable manipulators with different configurations are applied to verify the effectiveness of the proposed control scheme in numerical simulation.

Keywords: Constrained reconfigurable manipulator, Force/position control, Joint torque estimation, Non-fragile robust control, Dynamic output feedback

1. Introduction

Free motion control and constrained motion control are two basic strategies in the control of reconfigurable manipulators. Most of the existing researches for reconfigurable manipulators are carried out under the space which was totally free of environment constraints [1-4]. Actually, in most practical applications such as polishing, grinding, crawling, assembling etc., the manipulator may inevitably contact environments or manipulating objects [5-6]. Hence, position/force control is an important research topic in the domain of reconfigurable manipulator, particularly for applications in human environments and space.

In recent literatures, some researchers have paid much attention on controlling constrained manipulators [7-10]. Hybrid position/force control and impedance control are two basic strategies in the position/force control of constrained manipulators. The objective of hybrid position/force controller is to track a position (and orientation) trajectory in the position subspace and a force (and moment) trajectory in the force subspace. The impedance control of robot manipulators is to adjust the end-effector position in response to satisfy the target impedance behavior. In [11], a hybrid position/force trajectories control method for a robot manipulator interacting with a stiff environment is offered. A robust adaptive hybrid force/position control method for robot manipulators is presented in [12]. A force and position control method of parallel kinematic machines is discussed in [13], meanwhile, the artesian space computed torque control is applied to achieve force and position servoing directly in the task space. In [14], an impedance control strategy is presented to regulate both position and contact force of a piezoelectric−bimorph microgripper for micromanipulation and microassembly applications. In [15], continuum manipulator is designed to operate in constrained environments that are often unknown or unsensed, relying on body compliance to conform to obstacles. However, the aforementioned methods have been concentrated on the centralized control. For practical purposes, a centralized controller designed on the basis of an entire system may not be applicable for reconfigurable manipulators system due to its high computation costs, robustness, and complexities. Compared with centralized control, decentralized control scheme is more suitable for reconfigurable manipulators as it can effectively reduce the computational burden of centralized control structure. It should be stressed that, how to obtain each joint torque of constrained reconfigurable manipulator is a crucial issue for the purpose of achieving force decentralized control. Several techniques of direct joint torque sensing are proposed in the literatures [16-18]. However, using joint torque sensor measurements directly is known with many drawbacks and may degrade the reliability, ruggedness and simplicity of robot manipulators. Most robot manipulators are not equipped with joint torque sensor, and it is difficult

† Corresponding Author: Department of Control Science and Engineering, Changchun University of Technology, Changchun, China. (liyc@ccut.edu.cn)
* Department of Control Science and Engineering, Changchun University of Technology, Changchun, China. (zhoufandyouxiang@sina.com, dongbo@ccut.edu.cn)
Received: May 10, 2016; Accepted: July 27, 2017

to add them due to mechanical design constraints. To avoid these problems, this paper proposes a novel decentralized force/position control method for constrained reconfigureable manipulators without using torque sensor.

Feedback control is predominantly considered as an effective technique for improving the performance of controller [19-20]. Due to the states of system are not always available in practical situations, the output feedback control method is developed. Compared with the state feedback control, output feedback control problem is more challenging because of the limited information of state variables. The output feedback can be classified into two categories: static output feedback and dynamic output feedback. It is well known that the static output feedback is easy for implementation, but some strict conditions should be imposed on the system. Hence, the dynamic output feedback technique is more flexible and the required conditions on the considered systems are less conservative. In [21], a decentralized dynamic output feedback based linear controller is presented, where the feedback gain matrices of local controllers are obtained by solving an optimization problem subject to linear matrix inequalities. In [22], the finite-time dynamic output feedback controllers have been designed for linear stochastic systems and stochastic retarded systems. A discrete event-triggering mechanism is presented in [23] to determine whether or not a sampled signal packet will be transmitted for dynamic output feedback controller design. However, the controller coefficient sensitivity is not taken into account in the aforementioned papers. It's worth noting that relatively small perturbation of controller parameters might lead to instability of the reconfigurable manipulator system. Non-fragile control strategy is a well-known robust control approach for systems with perturbation of controller parameters [24-25]. In this work, a non-fragile robust technique is introduced into dynamic output feedback controller to solve the problem of parameter perturbation of the controller. Moreover, a novel decentralized position/force controller is designed by combining the joint torque estimation method and the non-fragile dynamic output feedback technique. Finally, the stability of the closed-loop system is proved by using Lyapunov theory and linear matrix inequality (LMI) technique.

The major contributions of this paper can be summarized as follows. (i) it extends the position tracking control to position/force tracking control, which adapts to the increasing demands of reconfigurable manipulator contact to task environments; (ii) unlike previous position/force control which are focused on position decentralized control, this paper takes into account the decentralized control of position and constraint force simultaneously, which has wider application potentials; (iii) The influence of controller parameter perturbation is reduced by introducing a non-fragile robust method into dynamic output feedback controller.

The rest of this paper is organized as follows. The harmonic drive mechanism and the torque estimation algorithm are described in Section 2. The nonlinear interconnected subsystem dynamic model of constrained reconfigurable manipulator is described in Section 3. The non-fragile robust dynamic output feedback controller is designed and the stability proof is illustrated in detail based on Lyapunov theory in Section 4. The effectiveness of the presented method is verified by the numerical simulation results of two 2-DOF reconfigurable manipulators with different configurations in Section 5. Some conclusions are drawn in Section 6.

2. Torque Estimation Mechanism

Considering the constrained reconfigurable module manipulator consists of n-modules, each module provides an independently rotating joint with harmonic drive transmission. The graph in Fig. 1 depicts the main components of harmonic drives. The wave generator (WG) is connected to a motor, the circular spline (CS) is connected to the joint base, and the flexspline (FS) is sandwiched in between the CS and the WG and connected to the joint output [26].

Owing to flexibility of FS and WG, a kinematic representation of a harmonic drive is illustrated in Fig. 2.

Therefore, FS and WG torsion are defined as follows:

$$\Delta\theta_{fi} = \theta_{foi} - \theta_{fsi} \tag{1}$$

Fig. 1. Exploded view of a harmonic drive showing the three components

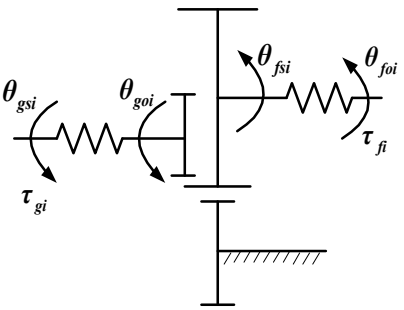

Fig. 2. Kinematic representation of a harmonic drive showing the three ports

$$\Delta\theta_{gi} = \theta_{goi} - \theta_{gsi} \tag{2}$$

where θ_{fsi} and θ_{foi} denote the angular position at the flexspline gearside (gear-toothed circumference) and the flexspline angular position at the load side which is measured using the link-side encoder, respectively. θ_{goi} and θ_{gsi} denote the positions of the wave generator outside part (ball bearing outer rim) and the center part (wave generator plug), respectively.

When considering the compliance of wave generator, the angular positions at the components of the harmonic drive, as explained in [27], can be obtained by using the input/ output kinematic relationship as:

$$\theta_{gsi} = -\delta_i \theta_{fsi} \tag{3}$$

When the harmonic drive torsion is assumed to be caused by flexspline only, the harmonic drive torsion can be obtained by using the following expression:

$$\Delta\theta_i = \theta_{foi} - \theta_{fsi} = \theta_{foi} + \frac{\theta_{gsi}}{\delta_i} \tag{4}$$

By adding and subtracting the terms θ_{fsi} and θ_{goi} to (4), one obtains:

$$\begin{aligned}\Delta\theta_i &= \theta_{foi} - \theta_{fsi} + \left(\theta_{fsi} + \frac{\theta_{goi}}{\delta_i}\right) - \left(\frac{\theta_{goi}}{\delta_i} - \frac{\theta_{gsi}}{\delta_i}\right) \\ &= \Delta\theta_{fi} - \Delta\theta_{gi}/\delta_i + \theta_{erri}\end{aligned} \tag{5}$$

Where θ_{erri} denotes the kinematic error of harmonic drive transmission. Based on the assumption that there is no relative motion between the wave generator output and the flexspline input, we have $\theta_{erri} = 0$.

In order to model the harmonic drive compliance, consider its mechanical system analogy two-spring system [26]. As indicated in Fig. 3, the local elastic coefficient increases with the increase of τ_{fs}. Let us define the local elastic coefficient L_{fk} as:

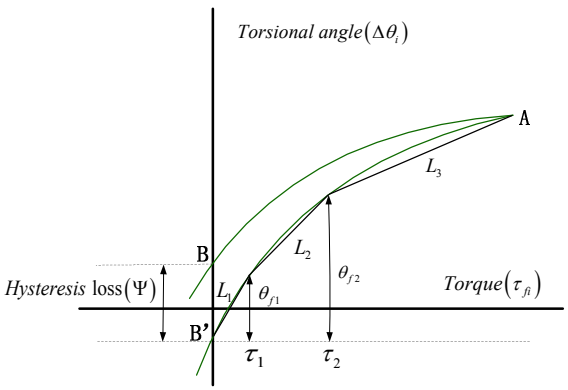

Fig. 3. Typical stiffness and hysteresis curve of a harmonic drive

$$L_{fk} = \frac{d\tau_{fi}}{d\Delta\theta_{fi}} \tag{6}$$

Considering the symmetry property of the flexspline stiffness and using Taylor expansion, the local elastic coefficient is approximated by:

$$L_{fk} = L_{fo}\left(1 + \left(a_f \tau_{fi}\right)^2\right) \tag{7}$$

Where L_{fo} and a_f are constants to be determined. If $L_{fo} \neq 0$, then the flexspline torsion can be calculated as:

$$\Delta\theta_{fi} = \int_0^{\tau_{fi}} \frac{d\tau_{fi}}{L_{fk}} \tag{8}$$

Substituting L_{fk} of (7) into (8), we obtain:

$$\Delta\theta_{fi} = \frac{arctan\left(a_f \tau_{fi}\right)}{a_f L_{fo}} \tag{9}$$

where $\arctan(\bullet)$ is the arctangent function. As show in Fig. 3, the harmonic drive torsional deformation can range from $-\Psi/2$ to $-\Psi/2$ at zero torque output, but drops down to zero at rated torque, where Ψ is the hysteresis loss. In order to replicate the hysteresis shape of this stiffness curve, the local elastic coefficient of wave generator is modeled as:

$$L_{gk} = L_{go} e^{a_g |\tau_{gi}|} \tag{10}$$

Where L_{go} and a_g are constants to be determined. If $L_{go} \neq 0$, then the wave generator torsional angle can be calculated using the following relation:

$$\Delta\theta_{gi} = \int_0^{\tau_{gi}} \frac{d\tau_{gi}}{L_{gk}} \tag{11}$$

Substituting L_{gk} of (10) into (11), we obtain:

$$\Delta\theta_{gi} = \int_0^{\tau_{gi}} \frac{d\tau_{gi}}{L_{gk}} = \frac{sign\left(\tau_{gi}\right)}{a_g L_{go}}\left(1 - e^{-a_g|\tau_{gi}|}\right) \tag{12}$$

Finally, by substituting the FS and WG deformation given in (9) and (12) into (5), the total deformation of the harmonic drive can be expressed as::

$$\Delta\theta_i = \frac{arctan\left(a_f \tau_{fi}\right)}{a_f} - \frac{sign\left(\tau_{gi}\right)}{a_g \delta_i L_{go}}\left(1 - e^{-a_g|\tau_{gi}|}\right) \tag{13}$$

Then,

$$\tau_{fi}=\frac{1}{a_f}tan\left(a_f L_{fo}\left(\Delta\theta_i+\frac{sign\left(\tau_{gi}\right)}{a_g\delta_i L_{go}}\left(1-e^{-a_g|\tau_{gi}|}\right)\right)\right) \quad (14)$$

where the wave generator torque τ_{gi} can be approximated by the motor torque command.

By the following formula, one can get the constrained torque which is obtained by the constrained force on the end-effector of manipulator:

$$\tau_{ci}=\tau_{fie}-\tau_{fio} \quad (15)$$

where τ_{fio} denotes the joint torque which is obtained in free space, τ_{fie} denotes the total joint torque in the constrained space. The total joint torque τ_{fie} and/or joint torque in free space τ_{fio} are directly obtained from formula (14) under the condition of constrained space and free space, respectively.

3. Problem Description

For a constrained reconfigurable manipulator, the motion of end-effector is constrained by its task environment. The constraint equation can be described as:

$$\phi(q)=0 \quad (16)$$

Under the environment constraint, the dynamic model of constrained reconfigurable manipulator with n-DOF can be described as follows:

$$M(q)q+C(q,q)q+G(q)+F\left(q,q\right)=u+\tau_c \quad (17)$$

where $q\in R^n$ is the vector of joint displacements, $M(q)\in R^{n\times n}$ is the symmetric and positive definite inertia matrix, $C(q,q)\in R^n$ is the matrix of centripetal Coriolis matrix, $G(q)\in R^n$ is the gravity vector, $u\in R^n$ is the control torque of output side in harmonic drive transmission, $F\left(q,q\right)\in R^n$ denotes the joint friction force item, $\tau_c\in R^n$ is the constrained torque which obtained by workspace force.

In the multidegree-of-freedom manipulator, the constrained torque vector for all joint τ_c relates to the constrained force on the end-effector of manipulator f as follows:

$$\tau_c=J_\Phi^T(q)f \quad (18)$$

where $J_\Phi^T(q)\in R^{m\times n}$ is the Jacobian matrix. f denotes the constrained force on the end-effector of manipulator.

As the complexity of the reconfigurable manipulators system grew with the increase of the number of dof of the system model, how to realize decentralized force/position control is substantial important for reconfigurable manipulator [28-30]. Considering each of the joint module as a subsystem, the dynamics of module i can be expressed as:

$$\begin{aligned}&M_i(q_i)\ddot{q}_i+C_i(q_i,q_i)\dot{q}_i+G_i(q_i)\\&+F_i\left(q_i,\dot{q}_i\right)+Z_i(q,\dot{q},\ddot{q})=u_i+\tau_{ci}\\&Z_i(q,\dot{q},\ddot{q})=\left\{\sum_{j=1,j\neq i}^{n}M_{ij}(q)\ddot{q}_j+[M_{ii}(q)-M_i(q_i)]\ddot{q}_i\right\}\\&+\left\{\sum_{j=1,j\neq i}^{n}C_{ij}(q,\dot{q})\dot{q}_j+[C_{ii}(q,\dot{q})-C_i(q_i,\dot{q}_i)]\dot{q}_i\right\}\\&+[\bar{G}_i(q)-G_i(q_i)]\end{aligned} \quad (19)$$

where q_i, $\dot{q}_i$, $\ddot{q}_i$, $\bar{G}_i(q_i)$, $F_i(q_i,\dot{q}_i)$, u_i and τ_{ci} are the i th element of the vectors q, $\dot{q}$, $\ddot{q}$, $G(q)$, $F(q,\dot{q})$, u and τ_c, respectively. $M_{ij}(q)$ and $C_{ij}(q,\dot{q})$ are the ij th element of the matrices $M(q)$ and $C(q,\dot{q})$, respectively.

The constrained reconfigurable manipulator dynamic model of nonlinear interconnected subsystem S_i can be presented by the following state equation:

$$S_i:\begin{cases}\dot{x}_i=A_ix_i+B_i[f_i(q_i,\dot{q}_i)\\\qquad+g_i(q_i)(u_i+\tau_{ci})+h_i(q,\dot{q},\ddot{q})]\\y_i=C_ix_i\end{cases} \quad (20)$$

where $x_i=[x_{i1},x_{i2}]^T=[q_i,\dot{q}_i]^T,(i=1,2,...,n)$ is the state vector of subsystem S_i, and y_i is the output of subsystem S_i. The matrices:

$$\begin{aligned}&A_i=\begin{bmatrix}0&1\\0&0\end{bmatrix},\ B_i=\begin{bmatrix}0\\1\end{bmatrix},\ C_i=\begin{bmatrix}1&0\\0&1\end{bmatrix},\\&f_i(q_i,\dot{q}_i)=M_i^{-1}(q_i)\left[-C_i(q_i,\dot{q}_i)\dot{q}_i-G_i(q_i)-F_i(q_i,\dot{q}_i)\right],\\&g_i(q_i)=M_i^{-1}(q_i),\\&h_i(q,\dot{q},\ddot{q})=-M_i^{-1}(q_i)Z_i(q,\dot{q},\ddot{q})\end{aligned}$$

The control objective is to design a decentralized position/force control scheme for Eq. (20) to make sure that the actual position q and the contact force f of the reconfigurable manipulator can follow their desired trajectories.

4. Control Design and Stability Analysis

In this section, a non-fragile robust dynamic output feedback controller with additive gain variations is designed to insure the asymptotic stability of the reconfigurable manipulator system as well as satisfying a predefined H_∞ performance level. Based on the Lyapunov theory, the

proving process of the proposed control method is presented.

An augmented system consisting of the system (20) and the integral of the tracking error ($e_{ti} = \int y_{id} - y_i$) is defined as follows:

$$\begin{cases} \dot{\overline{x}}_i = \overline{A}_i \overline{x}_i + \overline{B}_i [f_i(q_i, \dot{q}_i) + g_i(q_i)(u_i + \tau_{ci}) \\ \qquad\qquad + h_i(q,\dot{q},\dot{q})] + R_i y_{id} \\ \overline{y}_i = \overline{C}_i \overline{x}_i \end{cases} \tag{21}$$

where

$$\overline{A}_i = \begin{bmatrix} 0 & -C_i \\ 0 & A_i \end{bmatrix},\ \overline{x}_i = \begin{bmatrix} e_{ti} \\ x_i \end{bmatrix},\ \overline{B}_i = \begin{bmatrix} 0 \\ B_i \end{bmatrix},$$
$$R_i = \begin{bmatrix} I \\ 0 \end{bmatrix},\ \overline{C}_i = \begin{bmatrix} I & 0 \\ 0 & C_i \end{bmatrix}$$

Assumption 1: The desired trajectories q_{id} , $\dot{q}_{id}$ and $\ddot{q}_{id}$ are bounded.

Assumption 2: The rigid environmental constraints completely known. Moreover, the end-effector and constraint surface contact all the time, as well as the friction between them is ignored.

Assumption 3: The reconfigurable manipulator stays away from singularities to ensure Jacobian matrix full rank.

Next, the RBF neural network with appropriate dimension is employed to approximate the nonlinear term $f_i(q_i, \dot{q}_i)$ and $g_i(q_i)$ as follows [29]:

$$f_i(q_i, \dot{q}_i, W_{if}) = W_{if}^T \Phi_{if}(q_i, \dot{q}_i) + \varepsilon_{if} \quad \|\varepsilon_{if}\| \le \varepsilon_1 \tag{22}$$

$$g_i(q_i, W_{ig}) = W_{ig}^T \Phi_{ig}(q_i) + \varepsilon_{ig} \quad \|\varepsilon_{ig}\| \le \varepsilon_2 \tag{23}$$

where W_{if} and W_{ig} are the ideal neural network weights, $\Phi(\bullet)$ is the neural network basis function, ε_{if} and ε_{ig} are the neural network approximation errors. ε_1 , ε_2 are known constants.

Defining $\hat{W}_{if}$ and $\hat{W}_{ig}$ .as the estimations of W_{if} and W_{ig} , respectively. $\hat{f}_i(q_i, \dot{q}_i, \hat{W}_{if})$ is estimation value of $f_i(q_i, \dot{q}_i, W_{if})$ and $\hat{g}_i(q_i, \hat{W}_{ig})$ is estimation value of $g_i(q_i, W_{ig})$. $\hat{f}_i(q_i, \dot{q}_i, \hat{W}_{if})$ and $\hat{g}_i(q_i, \hat{W}_{ig})$ can be expressed as:

$$\hat{f}_i(q_i, \dot{q}_i, \hat{W}_{if}) = \hat{W}_{if}^T \Phi_{if}(q_i, \dot{q}_i) \tag{24}$$

$$\hat{g}_i(q_i, \hat{W}_{ig}) = \hat{W}_{ig}^T \Phi_{ig}(q_i) \tag{25}$$

Define the estimation errors as $W_{if} = W_{if} - \hat{W}_{if}$ and $W_{ig} = W_{ig} - \hat{W}_{ig}$. Therefore,

$$f_i(q_i, \dot{q}_i, W_{if}) - \hat{f}_i(q_i, \dot{q}_i, \hat{W}_{if}) = \tilde{W}_{if}^T \Phi_{if}(q_i, \dot{q}_i) + \varepsilon_{if} \tag{26}$$

$$g_i(q_i, W_{ig}) - \hat{g}_i(q_i, \hat{W}_{ig}) = \tilde{W}_{ig}^T \Phi_{ig}(q_i) + \varepsilon_{ig} \tag{27}$$

Property [31]: Boundedness of the interconnection term $h_i(q, \dot{q}, \ddot{q})$ for reconfigurable manipulator system:

$$\left\| h_i(q, \dot{q}, \ddot{q}) \right\| \le \sum_{j=1}^{n} d_{ij} Q_j \tag{28}$$

Where $Q_i = 1 + \|q_j\| + \|\dot{q}_j\| + \ldots + \|q_j\|^p + \|\dot{q}_j\|^p$, $d_{ij} \ge 0$, $p \ge 1$.

Similarly, using the RBF neural networks to approximate the interconnection term as follows:

$$h_i(|x_{ie}|, W_{ih}) = W_{ih}^T \Phi_{ih}(|x_{ie}|) + \varepsilon_{ih} \quad \|\varepsilon_{ih}\| \le \varepsilon_3 \tag{29}$$

where the W_{ih} is the ideal neural network weights, Φ_{ih} is the neural network basis function, ε_{ih} is the neural network approximation errors, ε_3 is known constant.

Define $\hat{W}_{ih}$ and $\hat{\Phi}_{ih}$ as the estimations of W_{ih} and Φ_{ih} . $\hat{h}_i(|x_{ie}|, \hat{W}_{ih})$ is the estimation value of $h_i(|x_{ie}|, W_{ih})$ and it can be expressed as:

$$\hat{h}_i(|x_{ie}|, \hat{W}_{ih}) = \hat{W}_{ih}^T \Phi_{ih}(|x_{ie}|) \tag{30}$$

Define the estimation errors as $W_{ih} = W_{ih} - \hat{W}_{ih}$. Then, one obtained that:

$$h_i(|x_{ie}|, W_{ih}) - \hat{h}_i(|x_{ie}|, \hat{W}_{ih}) = \tilde{W}_{ih}^T \Phi_{ih}(|x_{ie}|) + \varepsilon_{ih} \tag{31}$$

Defining the approximation error as:

$$\omega_{i1} = \varepsilon_{if} + \varepsilon_{ig}(u_i + \tau_{ci}) \tag{32}$$

$$\omega_{i2} = \varepsilon_{ih} \tag{33}$$

$$\omega_i = |\omega_{i1}| + |\omega_{i2}| \tag{34}$$

In order to approximate the performance index function, the weight vector should be updated as:

$$\dot{\hat{W}}_{if} = \eta_{if}(Y\overline{B}_i \overline{x}_i - N\overline{B}_i x_{ic}) \Phi_{if}(q_i, \dot{q}_i) \tag{35}$$

$$\dot{\hat{W}}_{ig} = \eta_{ig}(Y\overline{B}_i \overline{x}_i - N\overline{B}_i x_{ic}) \Phi_{ig}(q_i)(u_i + \tau_{ci}) \tag{36}$$

$$\dot{\hat{W}}_{ih} = \eta_{ih}(Y\overline{B}_i \overline{x}_i - N\overline{B}_i x_{ic}) \Phi_{ih}(x_{ie}) \tag{37}$$

$$\dot{\hat{\omega}}_i = \lambda_i(Y\overline{B}_i \overline{x}_i - N\overline{B}_i x_{ic}) \tag{38}$$

where η_{if} , η_{ig} , η_{ip} and λ_i are positive constants.

Assumption 4: The error between joint constrained torque estimated value and its actual value is small enough so that it can be ignored.

Considering the augmented constrained subsystems dynamic model (21), the decentralized non-fragile robust dynamic output feedback controller is designed as follows:

$$\begin{cases} \dot{x}_{ic} = A_{\Delta i} x_{ic} + B_{\Delta i} \overline{y}_i \\ u_i = \dfrac{1}{\hat{g}_i\left(q_i, \hat{W}_{ig}\right)} \begin{bmatrix} C_{\Delta i} x_{ic} + D_{\Delta i} \overline{y}_i \\ -\hat{f}_i\left(q_i, \dot{q}_i, \hat{W}_{if}\right) \\ -\hat{p}_i\left(|e_i|, \hat{W}_{ip}\right) + e_{\tau i} - \hat{\omega}_i \end{bmatrix} - \tau_{ci} \end{cases} \tag{39}$$

Remark: $A_{\Delta i} = A_{ic} + \Delta A_{ic}$, $B_{\Delta i} = B_{ic} + \Delta B_{ic}$
$C_{\Delta i} = C_{ic} + \Delta C_{ic}$, $D_{\Delta i} = D_{ic} + \Delta D_{ic}$

where A_{ic}, B_{ic}, C_{ic}, and D_{ic} are the nominal controller gain matrices to be determined. ΔA_{ic}, ΔB_{ic}, ΔC_{ic}, and ΔD_{ic} are unknown matrices representing norm-bounded controller gain variations, and are assumed to be satisfied:

$$\begin{aligned} \Delta A_{ic} &= L_{ia} F_{ia} M_{ia}, \quad \Delta B_{ic} = L_{ib} F_{ib} M_{ib}, \\ \Delta C_{ic} &= L_{ic} F_{ic} M_{ic}, \quad \Delta D_{ic} = L_{id} F_{id} M_{id} \end{aligned} \tag{40}$$

Where L_{ia}, L_{ib}, L_{ic}, L_{id}, M_{ia}, M_{ib}, M_{ic} and M_{id} are known real constant matrices of appropriate dimensions, and F_{ia}, F_{ib}, F_{ic}, F_{id} represents an unknown real-valued time-varying matrix satisfying:

$$F_{it}^T F_{it} \le I, \qquad t = a, b, c, d \tag{41}$$

Next, define the joint torque error as follows:

$$e_{\tau i} = \tau_{ci} - \tau_{di} \tag{42}$$

Combining Eq. (21) with Eq. (39), one can obtain that:

$$\begin{cases} \dot{x}_{ie} = A_{ie} x_{ie} + B_{ie} d_{ie} + \Delta G_i \\ \overline{y}_{ie} = C_{ie} x_{ie} \end{cases} \tag{43}$$

where $x_{ie} = \begin{bmatrix} \overline{x}_i \\ x_{ic} \end{bmatrix}$, $A_{ie} = \begin{bmatrix} \overline{A}_i + \overline{B}_i D_{\Delta i} \overline{C}_i & \overline{B}_i C_{\Delta i} \\ B_{\Delta i} \overline{C}_i & A_{\Delta i} \end{bmatrix}$,

$d_{ie} = \begin{bmatrix} e_{\tau i} \\ y_{id} \end{bmatrix}$, $B_{ie} = \begin{bmatrix} \overline{B}_i & R_i \\ 0 & 0 \end{bmatrix}$, $C_{ie} = \begin{bmatrix} \overline{C}_i & 0 \end{bmatrix}$,

$\Delta G_i = \begin{bmatrix} \overline{B}_i \left[\left(f_i - \hat{f}_i\right) + \left(g_i - \hat{g}_i\right)\left(u_i + \tau_{ci}\right) + h_i - \hat{h}_i - \hat{\omega}_i \right] \\ 0 \end{bmatrix}$

Lemma1 [32]: For any appropriate dimensions constant matrices D, E and any scalar $\varepsilon > 0$, the following inequality holds:

$$D^T E + E^T D \le \varepsilon D^T D + \varepsilon^{-1} E^T E \tag{44}$$

Lemma2 [33] (Schur Complement Formula): For block matrix $A = \begin{bmatrix} A_{11} & A_{12} \\ A_{12}^T & A_{22} \end{bmatrix}$, the following conditions are proved to be equivalent:

$$(1) \quad A < 0 \tag{45}$$

$$(2) \quad A_{11} < 0, A_{22} - A_{12}^T A_{11}^{-1} A_{12} < 0 \tag{46}$$

$$(3) \quad A_{22} < 0, A_{11} - A_{12} A_{22}^{-1} A_{12}^T < 0 \tag{47}$$

Lemma3 [34]: In the given system, the eigenvalues of the system are located in a LMI region in the complex plane defined by $D(q,r)$ which is defined by merging different eigenvalues constraints to produce a $D(q,r)$ region in which q and r are the center and radius of the disc region. If there exist symmetric positive-definite matrices X and Y and matrices $A_{\Delta i}$, $B_{\Delta i}$, $C_{\Delta i}$, $D_{\Delta i}$, as well as the corresponding LMI such that:

$$\begin{bmatrix} X & I \\ I & Y \end{bmatrix} > 0 \tag{48}$$

$$\begin{bmatrix} A_{11} & A_{12} & \overline{B}_i & R_i & X\overline{C}_i^T & -X\overline{C}_i^T & 0 \\ A_{12}^T & A_{22} & Y\overline{B}_i & YR_i & \overline{C}_i^T & -\overline{C}_i^T & 0 \\ * & * & -\gamma_c^2 I & 0 & 0 & 0 & 1 \\ * & * & * & E^T E - \gamma_c^2 I & 0 & 0 & 0 \\ * & * & * & * & -I & 0 & 0 \\ * & * & * & * & * & -\varepsilon^{-1} & 0 \\ * & * & * & * & * & * & -\varepsilon \end{bmatrix} < 0 \tag{49}$$

where

$$A_{11} = \overline{A}_i X + X\overline{A}_i^T + \overline{B}_i \tilde{C}_{\Delta i} + \left(\overline{B}_i \tilde{C}_{\Delta i}\right)^T \tag{50}$$

$$A_{12} = A_{\Delta i}^T + \overline{A}_i + \overline{B}_i D_{\Delta i} \overline{C}_i \tag{51}$$

$$A_{22} = Y\overline{A}_i + \overline{A}_i^T Y + \tilde{B}_{\Delta i} \overline{C}_i + \left(B_{\Delta i} \overline{C}_i\right)^T \tag{52}$$

hold, the system is robust asymptotically stable and the H_∞ performance is guaranteed with an attenuation level γ.

The controller gains can be calculated by the following relation:

$$D_{\Delta i} = D_{\Delta i} \tag{53}$$

$$C_{\Delta i} = \left(C_{\Delta i} - D_{\Delta i} \overline{C}_i X\right) M^{-T} \tag{54}$$

$$B_{\Delta i} = N^{-1}\left(B_{\Delta i} - Y\overline{B}_i D_{\Delta i}\right) \tag{55}$$

$$\begin{aligned} A_{\Delta i} = N^{-1}\big[& A_{\Delta i} - Y\left(\overline{A}_i - \overline{B}_i D_{\Delta i} \overline{C}_i\right) X - \\ & Y\overline{B}_i C_{\Delta i} M^T - N B_{\Delta i} \overline{C}_i X \big] M^{-T} \end{aligned} \tag{56}$$

where M and N satisfy $MN^T = I - XY$.

Theorem. Based on Lemma3, given $\gamma > 0$ and constrained subsystems dynamic model (21), if there exist symmetric positive-definite matrices X and Y and matrices $A_{\Delta i}$, $B_{\Delta i}$, $C_{\Delta i}$ and $D_{\Delta i}$, as well as matrix LMI such that (49) holds, then system (21) is robust asymptotically stable

and satisfies the H_∞ performance indicator as follows:

$$\left\|\dot{e}_{ti}\right\|^2 \le \gamma^2 \left\|d_{ie}\right\|^2 + V(0) \tag{57}$$

where $\left\|\dot{e}_{ti}\right\|^2 = \int_0^{t_1} (\dot{e}_{ti}^T \dot{e}_{ti})dt$, $\left\|d_{ie}\right\|^2 = \int_0^{t_1} (d_{ie}^T d_{ie})dt$.

Proof: Choosing the Lyapunov candidate as $V_i = x_{ie}^T P_1 x_{ie}$, the time derivative of V_i along the trajectories of system (43) is:

$$\begin{aligned} V_i &= x_{ie}^T \left(A_{ie}^T P_1 + P_1 A_{ie}\right) x_{ie} + x_{ie}^T P_1 B_{ie} d_{ie} \\ &\quad + d_{ie}^T B_{ie}^T P_1 x_{ie} + \Delta G_i^T P_1 x_{ie} + x_{ie}^T P_1 \Delta G_i \\ &\quad - \eta_{if}^{-1} W_{if}^T \dot{\hat{W}}_{if} - \eta_{ig}^{-1} W_{ig}^T \dot{\hat{W}}_{ig} - \eta_{ih}^{-1} W_{ih}^T \dot{\hat{W}}_{ih} \\ &\quad - \lambda_i^{-1} \tilde{\omega}_i^T \dot{\hat{\omega}}_i \end{aligned} \tag{58}$$

Set $P_1 = \begin{bmatrix} Y & N \\ N^T & V \end{bmatrix}$, then:

$$\begin{aligned} \dot{V}_i &= x_{ie}^T \left(A_{ie}^T P_1 + P_1 A_{ie}\right) x_{ie} + x_{ie}^T P_1 B_{ie} d_{ie} \\ &\quad + d_{ie}^T B_{ie}^T P_1 x_{ie} + \left(Y\bar{B}_i \bar{x}_i - N\bar{B}_i x_{ic}\right) \\ &\quad \times \left[\tilde{W}_{if}^T \Phi_{if}(q_i, \dot{q}_i) + \tilde{W}_{ig}^T \Phi_{ig}(q_i)(u_i + \tau_{ci}) + \tilde{W}_{ih}^T \Phi_{ih}(|x_{ie}|) + \omega_i - \hat{\omega}_i\right] \\ &\quad - \eta_{if}^{-1} \tilde{W}_{if}^T \dot{\hat{W}}_{if} - \eta_{ig}^{-1} \tilde{W}_{ig}^T \dot{\hat{W}}_{ig} - \eta_{ih}^{-1} \tilde{W}_{ih}^T \dot{\hat{W}}_{ih} - \lambda_i^{-1} \tilde{\omega}_i^T \dot{\hat{\omega}}_i \\ &= x_{ie}^T \left(A_{ie}^T P_1 + P_1 A_{ie}\right) x_{ie} + x_{ie}^T P_1 B_{ie} d_{ie} \\ &\quad + d_{ie}^T B_{ie}^T P_1 x_{ie} + \tilde{W}_{if}^T \left[\left(Y\bar{B}_i \bar{x}_i - N\bar{B}_i x_{ic}\right) \Phi_{if}(q_i, \dot{q}_i) - \eta_{if}^{-1} \dot{\hat{W}}_{if}\right] \\ &\quad + \tilde{W}_{ig}^T \left[\left(Y\bar{B}_i \bar{x}_i - N\bar{B}_i x_{ic}\right) \right. \\ &\quad \left. \times \Phi_{ig}(q_i)(u_i + \tau_{ci}) - \eta_{ig}^{-1} \dot{\hat{W}}_{ig}\right] \\ &\quad + \tilde{W}_{ih}^T \left[\left(Y\bar{B}_i \bar{x}_i - N\bar{B}_i x_{ic}\right) \Phi_{ih}(|x_{ie}|) \right. \\ &\quad \left. - \eta_{ih}^{-1} \dot{\hat{W}}_{ih}\right] + \left(Y\bar{B}_i \bar{x}_i - N\bar{B}_i x_{ic}\right)(\omega_i - \hat{\omega}_i) \\ &\quad - \lambda_i^{-1} \tilde{\omega}_i^T \dot{\hat{\omega}}_i \end{aligned} \tag{59}$$

Substituting (35)-(37) into (59), yields the expression:

$$\begin{aligned} V_i &= x_{ie}^T \left(A_{ie}^T P_1 + P_1 A_{ie}\right) x_{ie} + x_{ie}^T P_1 B_{ie} d_{ie} \\ &\quad + d_{ie}^T B_{ie}^T P_1 x_{ie} + \left(Y\bar{B}_i \bar{x}_i - N\bar{B}_i x_{ic}\right) \\ &\quad \times (\omega_i - \hat{\omega}_i) - \lambda_i^{-1} \tilde{\omega}_i^T \dot{\hat{\omega}}_i \\ &= x_{ie}^T \left(A_{ie}^T P_1 + P_1 A_{ie}\right) x_{ie} + x_{ie}^T P_1 B_{ie} d_{ie} \\ &\quad + d_{ie}^T B_{ie}^T P_1 x_{ie} + \left(Y\bar{B}_i \bar{x}_i - N\bar{B}_i x_{ic}\right) \tilde{\omega}_i \\ &\quad - \lambda_i^{-1} \tilde{\omega}_i^T \dot{\hat{\omega}}_i \\ &= x_{ie}^T \left(A_{ie}^T P_1 + P_1 A_{ie}\right) x_{ie} + x_{ie}^T P_1 B_{ie} d_{ie} \\ &\quad + d_{ie}^T B_{ie}^T P_1 x_{ie} + \tilde{\omega}_i \left(Y\bar{B}_i \bar{x}_i - N\bar{B}_i x_{ic} - \lambda_i^{-1} \dot{\hat{\omega}}_i\right) \end{aligned} \tag{60}$$

By utilizing the adaptive laws (38), one has:

$$\dot{V}_i = x_{ie}^T \left(A_{ie}^T P_1 + P_1 A_{ie}\right) x_{ie} + x_{ie}^T P_1 B_{ie} d_{ie} + d_{ie}^T B_{ie}^T P_1 x_{ie} \tag{61}$$

Given the following index:

$$J = \int_0^{t_1} (\dot{e}_{ti}^T \dot{e}_{ti} - \gamma^2 d_{ie}^T d_{ie})dt$$

Thus,

$$\begin{aligned} J &= \int_0^{t_1} (\dot{e}_{ti}^T \dot{e}_{ti} - \gamma^2 d_{ie}^T d_{ie} + \dot{V})dt - \int_0^{t_1} \dot{V} dt \\ &= \int_0^{t_1} (\dot{e}_{ti}^T \dot{e}_{ti} - \gamma^2 d_{ie}^T d_{ie} + \dot{V})dt - V(t_1) + V(0) \\ &\le \int_0^{t_1} (\dot{e}_{ti}^T \dot{e}_{ti} - \gamma^2 d_{ie}^T d_{ie} + \dot{V})dt + V(0) \end{aligned} \tag{62}$$

where

$$\dot{e}_{ti}^T \dot{e}_{ti} = \left(y_{id} - \bar{y}_i\right)^T \left(y_{id} - \bar{y}_i\right) = y_{id}^T y_{id} - \bar{y}_i^T y_{id} - y_{id}^T \bar{y}_i + \bar{y}_i^T \bar{y}_i$$

Let $E = \begin{bmatrix} 0 & I \end{bmatrix}$, one can obtain:

$$\dot{e}_{ti}^T \dot{e}_{ti} = d_{ie}^T E^T E d_{ie} - d_{ie}^T E^T C_{ie} x_{ie} - x_{ie}^T C_{ie}^T E d_{ie} + x_{ie}^T C_{ie}^T C_{ie} x_{ie} \tag{63}$$

Based on Eq.(62), for achieve the required property index (59) and stability of the augmented system (39) the following inequality needs to be satisfied:

$$V_i + e_{ti}^T e_{ti} - \gamma^2 d_{ie}^T d_{ie} < 0 \tag{64}$$

By using Eq. (58), Eq. (63) and based on Lemma 2, inequality (64) means that the following formula must establish:

$$\begin{bmatrix} A_{ie}^T P_1 + P_1 A_{ie} & P_1 B_{ie} - C_{ie}^T E & C_{ie}^T \\ * & E^T E - \gamma^2 I & 0 \\ * & * & -I \end{bmatrix} < 0 \tag{65}$$

Inequality (65) can further decomposed as below:

$$\begin{aligned} &\begin{bmatrix} A_{ie}^T P_1 + P_1 A_{ie} & P_1 B_{ie} & C_{ie}^T \\ * & E^T E - \gamma^2 I & 0 \\ * & * & -I \end{bmatrix} + \\ &\begin{bmatrix} -C_{ie}^T \\ 0 \\ 0 \end{bmatrix} \begin{bmatrix} 0 & E & 0 \end{bmatrix} + \begin{bmatrix} 0 \\ E \\ 0 \end{bmatrix} \begin{bmatrix} -C_{ie}^T & 0 & 0 \end{bmatrix} < 0 \end{aligned} \tag{66}$$

On the basis of Lemma 1, inequality (66) is implied by the following formula:

$$\begin{bmatrix} A_{ie}^T P_1 + P_1 A_{ie} & P_1 B_{ie} & C_{ie}^T & -C_{ie}^T & 0 \\ * & E^T E - \gamma^2 I & 0 & 0 & E \\ * & * & -I & 0 & 0 \\ * & * & * & -\varepsilon^{-1} & 0 \\ * & * & * & * & -\varepsilon \end{bmatrix} < 0 \quad (67)$$

Set [35]:

$$F_1 = \begin{bmatrix} X & I \\ M^T & 0 \end{bmatrix}, \quad F_2 = \begin{bmatrix} I & Y \\ 0 & N^T \end{bmatrix}$$

then, it is clear to see that $F_1^T P_1 = F_2^T$.

Pre- and post-multiplying inequality (67) by $\begin{bmatrix} F_1^T & I & I & I & I \end{bmatrix}$ and its transpose respectively, yields:

$$\begin{bmatrix} F_1^T A_{ie}^T F_2 + F_2^T A_{ie} F_1 & F_2^T B_{ie} & F_1^T C_{ie}^T & -F_1^T C_{ie}^T & 0 \\ * & E^T E - \gamma^2 I & 0 & 0 & E \\ * & * & -I & 0 & 0 \\ * & * & * & -\varepsilon^{-1} & 0 \\ * & * & * & * & -\varepsilon^{-1} \end{bmatrix} < 0 \quad (68)$$

According to Eq. (53)-(56), it follows that (68) implies (49). Therefore, the system satisfies the H_∞ performance indicator and this completes the proof of Theorem.

5. Numerical simulations

To verify the effectiveness of the proposed non-fragile robust dynamic output feedback control strategy, in this subsection, two 2-DOF constrained reconfigurable manipulators with different configurations (see Fig.4) are employed.

Suppose the additive gain variations of the controller are expressed by Eq. (40) with:

$$L_{ai} = L_{bi} = \begin{bmatrix} 0.3 \\ 0.5 \\ -0.1 \\ 0.2 \end{bmatrix} \quad M_{ai} = M_{ci} = \begin{bmatrix} -0.2 & 0.4 & 0.1 & 0.3 \end{bmatrix}$$

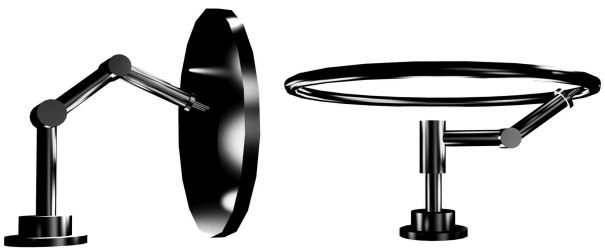

(a) (b)

Fig. 4. Configurations for simulation (a) configuration *a* (b) configuration *b*

$$L_{ci} = L_{di} = 0.1 \quad M_{ci} = M_{di} = \begin{bmatrix} 0.2 & 0.6 & 0.3 & 0.5 \end{bmatrix}$$
$$F_{ti} = I, \quad t = a,b,c,d \quad i = 1,2$$

By using YALMIP Toolbox [36] and selecting LMILab solver under the Matlab software, one can obtain the controller gain matrices listed below:

$$A_{1c} = A_{2c} = \begin{bmatrix} -10.3049 & -18.5541 & -1.0296 & -9.5123 \\ -0.4121 & -1.3049 & 0 & 0 \\ -0.3600 & 0 & -9.7638 & -1.4081 \\ -0.4759 & 0 & -1.7485 & -9.4442 \end{bmatrix}$$

$$B_{1c} = B_{2c} = \begin{bmatrix} -2.4495 & 3.4799 & 1.7963 & 3.8811 \\ 3.8811 & -2.4495 & -1.7963 & 3.8819 \\ 1.0297 & -1.0297 & -1.5868 & -0.5360 \\ 3.1680 & 0.1650 & -4.9985 & -8.7807 \end{bmatrix}$$

$$C_{1c} = C_{2c} = \begin{bmatrix} -0.6980 & 0.6980 & -0.5111 & -0.1360 \end{bmatrix}$$
$$D_{1c} = D_{2c} = \begin{bmatrix} 2.0889 & 2.0889 & -1.6513 & -365.30 \end{bmatrix}$$

For the sake of analyzing aforementioned configurations, a form of analytic diagram is offered in Fig. 5.

The control law (39) is applied to the whole control system and the initial position and velocity are set as $q_1(0) = q_2(0) = 1$ and $q_1(0) = q_2(0) = 0$, respectively. The control parameters are selected as $\eta_{if} = 0.002$, $\eta_{ig} = 0.002$, $\eta_{ih} = 500$, $\lambda_i = 0.002$ and the H_∞ performance indicator is defined as $\gamma = 1.0$.

Fig.4 (a) shows the planar graph of configuration a. It is assumed that the constrained reconfigurable manipulator is simulating a polishing task and the constraint equation can be depicted as:

$$\phi(q) = l_1 \cos(q_1) + l_2 \cos(q_2) - 1 = 0 \quad (69)$$

where $l_1 = 1$, $l_2 = 1$ are the lengths of the two robot links. The desired position and the desired constraint force are defined as:

$$q_{1d} = \cos(\pi t) + \sin(\pi t) \quad (70)$$

$$q_{2d} = \arccos\left(\frac{1 - l_1 \cos(q_{1d})}{l_2}\right) \quad (71)$$

$$f_d = 10N \quad (72)$$

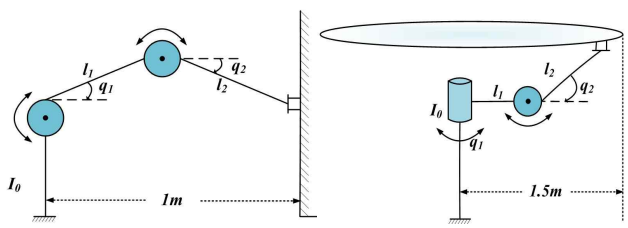

(a) (b)

Fig. 5. The analytic charts of the configurations: (a) Configuration *a*; (b) Configuration *b*

Position tracking trajectories and position tracking errors of configuration a are illustrated in Fig. 6 where the actual and desired trajectories are almost overlap. From Fig. 7, one can obtain that mapping the end contact force to joint space, the equivalent torque tracking errors can also converge to zero. Fig. 8 shows the tracking performance of the contact force and the force tracking error curves, in which the system converges to an error that can be considered as zero (less than 0.01 N). It can be concluded that high performance of the simultaneous position-force tracking is achieved with relatively smooth control effort.

In order to further check the effectiveness of the presented scheme for decentralized position/force control under different configurations, the same controller is used to configuration b. Fig. 4 (b) shows that the reconfigurable manipulator works in constrained environment such as cylinders. The constraint equation can be expressed as $\phi(q) = l_1 + l_2 \cos(q_2) - 1.5 = 0$. The desired position and the desired constraint force are defined as:

$$q_{1d} = \cos(2t) \tag{73}$$

$$q_{2d} = \frac{\pi}{3} \tag{74}$$

$$f_d = 6\ N \tag{75}$$

The parameters of the decentralized position/force controller in configuration b are chosen as those in configuration a. The position tracking performance, equivalent torque tracking performance and force tracking performance of configuration b are presented in Figs. 9-11, respectively. The numerical simulation results demonstrate that the presented decentralized position/force control strategy can be used to different configurations of constrained reconfigurable manipulators without changing any control parameters. This is an important and meaningful advantage for control the reconfigurable manipulators with a requirement of frequent conversion from one configuration to another in order to complete different kinds of tasks in

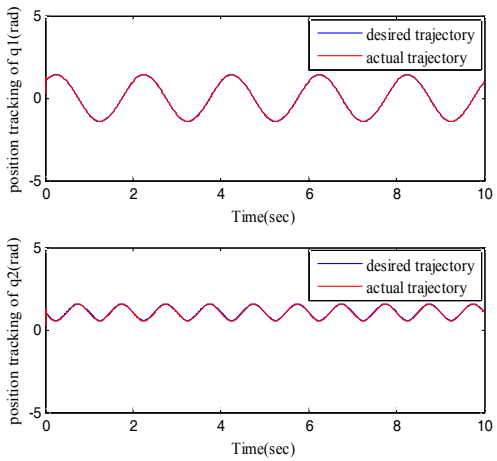

(a)

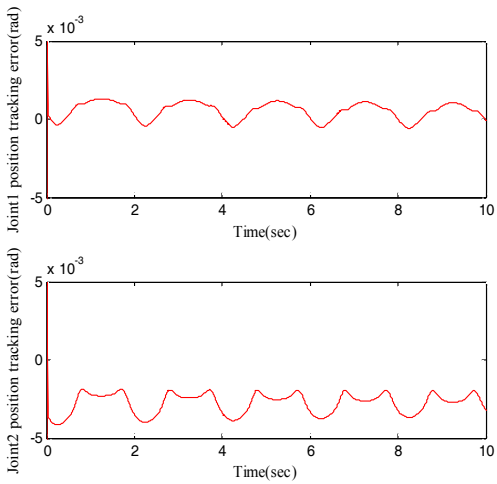

(b)

Fig. 6. (a) Position tracking performance of configuration a (b) Position tracking error of configuration a

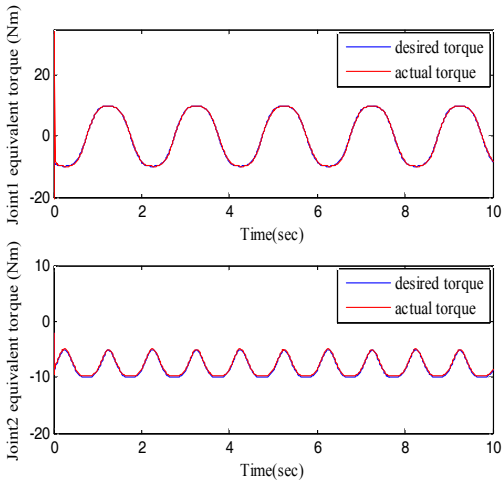

(a)

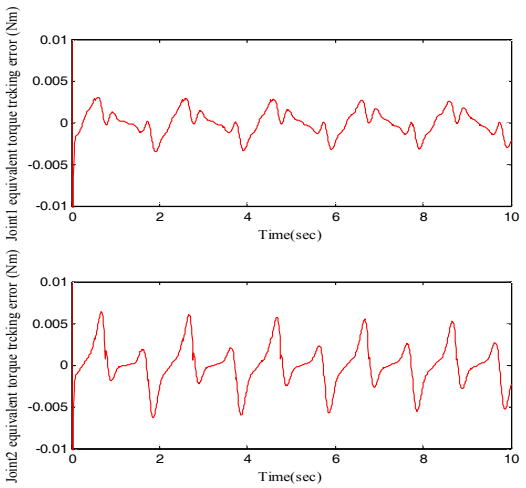

(b)

Fig. 7. (a) Equivalent torque of configuratio n a: (b) Equivalent torque tracking error of configuration a

different environment.

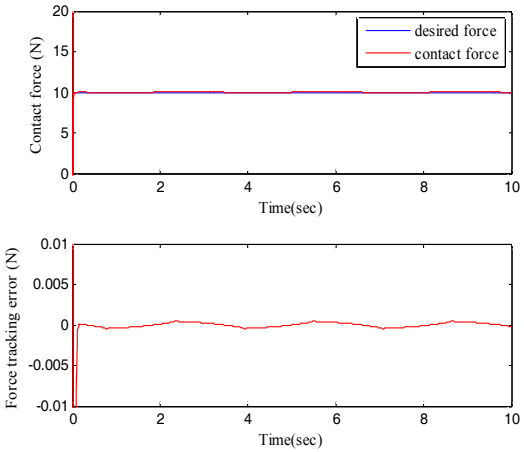

Fig. 8. Force tracking curves and force tracking error of configuration *a*

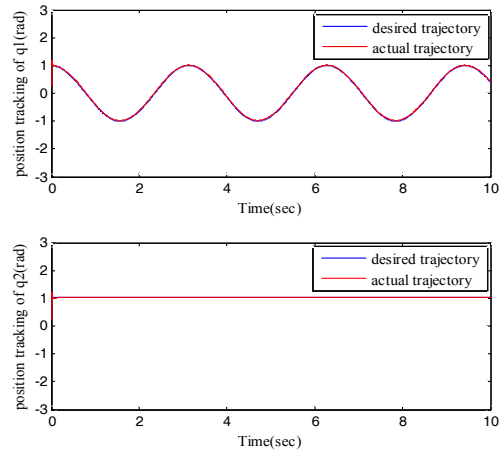

(a)

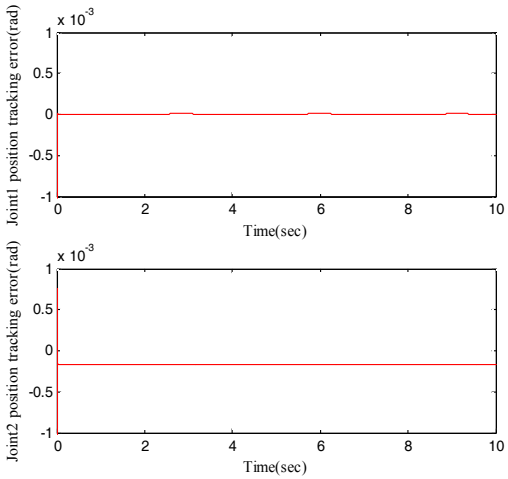

(b)

Fig. 9. (a) Position tracking performance of configuration *b*; (b) Position tracking error of configuration *b*

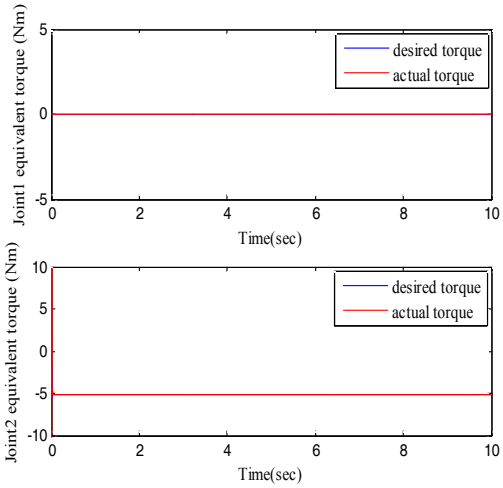

(a)

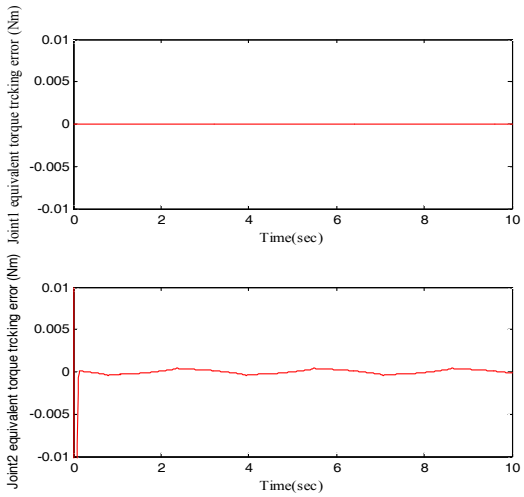

(b)

Fig. 10. (a) Equivalent torque of configuration *b* ; (b) Equivalent torque tracking error of configuration *b*

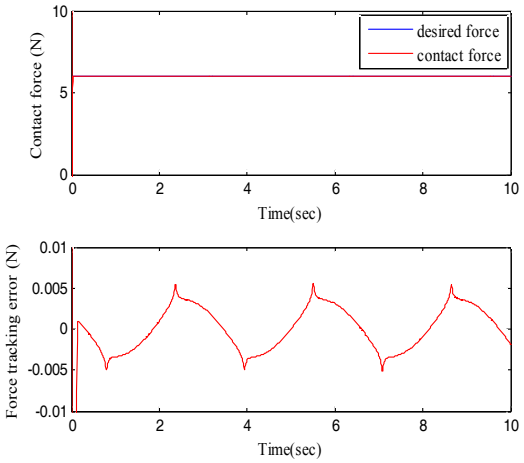

Fig. 11. Force tracking curves and force tracking error of configuration *b*

6. Conclusion

A torque sensorless decentralized position/force control scheme using dynamic output feedback technique was presented for constrained reconfigurable manipulator. Torque estimation based on position measurements provides an advantage of noise immunity to the estimated joint torque and reduces the cost of joint torque sensing. The influence of parameter perturbation of dynamic output feedback controller with additive gain variations has been reduced by introducing non-fragile robust method. Moreover, the stability of closed-loop system is proved using the Lyapunov theory and linear matrix inequality (LMI) technique. Finally, the effectiveness of the proposed scheme was verified under the conditions of different configurations without revising any parameters.

Acknowledgements

This work is financially supported by the National Natural Science Foundation of China (61374051 and 60974010) and Scientific and Technological Development Plan Project in Jilin Province of China (20160414033GH and 20160520013JH).

References

[1] M. Biglarbegian, W. Melek, and J.M. Mendel, "Design of novel interval type-2 fuzzy controllers for modular and reconfigurable robots: theory and experiments," *IEEE Transactions on Industrial Electronics*, vol. 58, no. 4, pp. 1371-1384, April 2011.

[2] G. Antonelli, F. Arrichiello, F. Caccavale, and A. Marino, "Decentralized time-varying formation control for multi-robot systems," *International Journal of Robotics Research*, vol. 33, no. 7, pp. 1029-1043, May 2014.

[3] Y. Liu, and G. Liu, "Interaction analysis and online tip-over avoidance for a reconfigurable tracked mobile modular manipulator negotiating slopes," *IEEE/ASME Transactions on Mechatronics*, vol. 15, no. 4, pp. 623-635, Aug. 2010.

[4] G. Liu, S. Abdul, and A.A Goldenberg, "Distributed control of modular and reconfigurable robot with torque sensing," *Robotica*, vol. 26, no. 1, pp. 75-84, January 2008.

[5] J. Wang, and Y. Li, "Manipulation of a mobile modular manipulator interacting with the environment with the assistance of tactile sensing feedback," *Intelligent Robotics and Applications*, vol. 6424, no. 6, pp. 214-225, Nov. 2010.

[6] Z. Kappassov, J.A. Corrales, and V. Perdereau, "Tactile sensing in dexterous robot hands — Review," *Robotics and Autonomous Systems*, vol. 74, no. PA, pp. 195-220, 2015.

[7] S.M.M. Rahman, and R. Ikeura, "Weight-prediction-based predictive optimal position and force controls of a power assist robotic system for object manipulation," *IEEE Transactions on Industrial Electronics*, vol. 63, no. 9, pp. 5964-5975, May 2016.

[8] Q. Xu, "Robust impedance control of a compliant microgripper for high-speed position/force regulation," *IEEE Transactions on Industrial Electronics*. Vol. 62, no. 2, pp. 1201-1209, Feb. 2015.

[9] Z. Li, X. Cao, Y. Tang, R. Li, and W. Ye, "Bilateral teleoperation of holonomic constrained robotic systems with time-varying delays," *IEEE Transactions on Instrumentation and Measure,* vol. 62, no. 4, pp. 752-765, April 2013.

[10] C. Lee, and W. Wang, "Robust adaptive position and force controller design of robot manipulator using fuzzy neural networks," *Nonlinear Dynamic*, vol. 85, no. 1, pp. 343-354, March 2016.

[11] D. Heck, A. Saccon, N. Wouw, and H. Nijmeijer, "Guaranteeing stable tracking of hybrid position-force trajectories for a robot manipulator interacting with a stiff environment," *Automatica,* vol. 63, pp. 235-247, 2016

[12] H.P. Singh, and N. Sukavanam, "Stability analysis of robust adaptive hybrid position/force controller for robot manipulators using neural network with uncertainties," *Neural Computing and Applications,* Vol. 22, no. 7-8, pp. 1745-1755, June 2013.

[13] S. Bellakehal, N. Andreff, Y. Mezouar, and M. Tadjine, "Vision/force control of parallel robots," *Mechanism and Machine Theory,* vol. 46, no. 10, pp. 1376-1395, 2011.

[14] Q. Xu, "Adaptive discrete-time sliding mode impedance control of a piezoelectric microgripper," *IEEE Transactions on Robotics*, vol. 19, no. 3, pp. 663-673, June 2013.

[15] M.C. Yip, and D.B. Camarillo, "Model-less hybrid position/force control: a minimalist approach for continuum manipulators in unknown, constrained environments," *IEEE Robotics and Automation Letters*, vol. 1, no. 2, pp. 844-851, Feb. 2016.

[16] A. Albu-Schaffer, C. Ott, and G. Hirzinger, "A unified passivity-based control framework for position, torque and impedance control of flexible joint robots," *Int Journal Robot Res,* vol. 26, no. 1, 23-39, January 2007.

[17] G. Liu, Y. Liu, and A.A. Goldenberg, "Design, analysis, and control of a spring-assisted modular and reconfigurable robot," *IEEE/ASME Trans Mechatronics*, vol. 16, no. 4, pp. 695-706, August 2011.

[18] M. Fumagalli, S. Ivaldi, M. Randazzo, L. Natale, G.Metta, G. Sandini and F. Nori, "Force feedback exploiting tactile and proximal force/torque sensing," Autonomous Robots, vol. 33, no. 4, pp. 381-398, April 2012.

[19] S. Islam, and P.X. Liu, "PD output feedback control design for industrial robotic manipulators," *IEEE/ASME Transactions on Mechatronics,* vol. 16, no. 1, pp. 187-197, Feb. 2011.
[20] L. Wen, T.M. Wang, G.H. Wu, and J.H. Liang, "Hydrodynamic investigation of a self-propelled robotic fish based on a force-feedback control method," *Bioinspiration and Biomimetics*, vol. 7, no. 3, pp. 385-390, May 2012.
[21] K. Kalsi, J. Lian, and S.H. Zak, "Decentralized dynamic output feedback control of nonlinear interconnected systems," *IEEE Transactions on Automatic Control,* vol.55, no.8, pp.1964-1970, August 2010.
[22] X. M. Zhang, and Q. L. Han, "Event-triggered dynamic output feedback control for networked control systems," *Iet Control Theory and Applications,* vol. 8, no. 4, pp. 226-234, June 2014.
[23] Y. Chen, H. Zou, R. Lu, and A. Xue, "Finite-time stability and dynamic output feedback stabilization of stochastic systems," *Circuits, Systems, and Signal Processing*, vol. 33, no. 1, pp. 53-69, January 2014.
[24] X.H. Chang, and G.H. Yang "Nonfragile filtering of continuous-time fuzzy systems," *IEEE Transactions on Signal Processing*, vol. 59, no. 4, pp. 1528-1538, April 2011.
[25] K. Sivaranjani, R. Rakkiyappan, S. Lakshmanan, C.P. Lim, "Robust non-fragile control for offshore steel jacket platform with nonlinear perturbations," *Nonlinear Dynamics*, vol. 81, no. 4, pp. 2043-2057, September 2015.
[26] H. Zhang, S. Ahmad, and G. Liu, "Modeling of torsional compliance and hysteresis behaviors in harmonic drives," *IEEE/ASME Transactions on Mechatronics,* vol. 20, no. 1, pp. 178-185, Feb. 2015.
[27] H. D. Technologies, "CSD and SHD ultra-flat component sets and gearheads," *Harmonic Drive Technologies*, Peabody, MA, USA, 2012.
[28] G. Leena, and G. Ray, "A set of decentralized PID controllers for an n-link robot manipulator," *Sadhana,* vol. 37, no. 3, pp. 405-423, June 2012.
[29] M.C. Zhu, and Y.C. Li, "Decentralized adaptive fuzzy sliding mode control for reconfigurable modular manipulators," *International Journal of Robust and Nonlinear Control*, vol. 20, no. 4, pp. 472-488, March 2010.
[30] B. Zhao, and Y. Li, "Local joint information based active fault tolerant control for reconfigurable manipulator," *Nonlinear Dynamics*, vol. 77, no. 3, pp. 859-876, August 2014.
[31] Y. Tang, M. Tomizuka, and G. Guerrero, "Decentralized robust control of mechanical systems," *IEEE Transactions on Automatic Control*, vol. 45, no. 4, pp. 771-775, April 2000.
[32] D. Ichalal, J. Ragot, and D. Maquin, "New fault tolerant control strategies for nonlinear Takagi-Sugeno systems," *Int. J. Appl. Math. Comput. Sci,* vol. 22, no. 1, pp. 197-210, March 2012.
[33] X. Chang, and G.H. Yang, "Non-fragile H_∞ filter design for discrete-time fuzzy systems with multiplicative gain variations," *Information Sciences*, vol. 266, pp. 171-185, May 2014.
[34] L. Li, and Y. Jia, "Non-fragile dynamic output feedback control for linear systems with time-varying delay," *Iet Control Theory and Applications*, vol. 3, no. 8, pp. 995-1005, August 2009.
[35] L.S. Bai, Z.H. Tian, and S.J. Shi, "Robust fault detection for a class of nonlinear time-delay system," *Journal of the Franklin Institute*, vol. 344, no. 6, pp. 873-888, September 2007.
[36] J. Lofberg YALMIP, "A toolbox for modeling and optimization in MATLAB," *Optimization*, pp. 284-289, 2004.

Fan Zhou received her B.S. and M.S. degrees from Changchun University of Technology, China in 2012 and 2015, respectively. She is currently working towards a Ph.D. degree in the Department of Control Engineering, Changchun University of Technology, China. Her research interests include intelligent mechanical, robot control, and robust control.

Bo Dong received his M.S. and Ph.D degrees from Jilin University, China in 2012 and 2015, respectively. He is currently a postdoctoral fellow in State Key Laboratory of Management and Control for Complex Systems, Institute of Automation, Chinese Academy of Sciences, Beijing, China. His research interests include intelligent mechanical and robot control.

Yuan-Chun Li received his M.S. and Ph.D degrees from Harbin Institute of Technology, China in 1987 and 1990, respectively. He is currently a Professor in Changchun University of Technology, China. He is also a Professor in Jilin University, China. His research interest covers complex system modeling, intelligent mechanical, and robot control.